Bell nonlocality and fully-entangled fraction measured in an entanglement-swapping device without quantum state tomography: Supplemental Material

Karol Bartkiewicz,[1,2,*] Karel Lemr,[2,†] Antonín Černoch,[3,‡] and Adam Miranowicz[1,§]

[1] *Faculty of Physics, Adam Mickiewicz University, PL-61-614 Poznań, Poland*
[2] *RCPTM, Joint Laboratory of Optics of Palacký University and Institute of Physics of Czech Academy of Sciences, 17. listopadu 12, 771 46 Olomouc, Czech Republic*
[3] *Institute of Physics of the Czech Academy of Sciences, Joint Laboratory of Optics of PU and IP AS CR, 17. listopadu 50A, 772 07 Olomouc, Czech Republic*

(Dated: February 9, 2017)

Here we describe additional experimental details including the maximum likelihood method, which ensures the positivity of the reconstructed correlation matrix R, the directly measured matrices (including the separable state $|VV\rangle$), and other methods related to the inseparable Werner states. We also plotted the measured values of the relevant entanglement witnesses. Moreover, we analyzed the efficiency for our method in comparison to quantum state tomography.

Hilbert-Schmidt representation and correlation matrix T

In our experiment we study photonic qubits encoded in polarization of single photons. The associated Pauli matrices are defined as $\sigma_1 = |D\rangle\langle D| - |A\rangle\langle A|$, $\sigma_2 = |L\rangle\langle L| - |R\rangle\langle R|$, $\sigma_3 = |H\rangle\langle H| - |V\rangle\langle V|$, where each capital letter corresponds to a particular polarization direction state (i.e., D for diagonal, A for antidiagonal, L for left-circular, R for right-circular, H for horizontal, and V for vertical polarizations).

A general two-qubit state can be expressed in the standard Hilbert-Schmidt form as

$$\rho = \frac{1}{4}\Big(I\otimes I + \vec{x}\cdot\vec{\sigma}\otimes I + I\otimes\vec{y}\cdot\vec{\sigma} + \sum_{i,j=1}^{3} T_{i,j}\,\sigma_i\otimes\sigma_j\Big), \quad (1)$$

where $\vec{\sigma} = [\sigma_1, \sigma_2, \sigma_3]$. The elements of the Bloch vectors read as $x_i = \mathrm{Tr}[\rho(\sigma_i \otimes I)]$ and $y_i = \mathrm{Tr}[\rho(I \otimes \sigma_i)]$, respectively. Finally, the correlation matrix T is defined as $T_{i,j} = \mathrm{Tr}[\rho(\sigma_i \otimes \sigma_j)]$ for $i, j = 1, 2, 3$.

Coincidence-count rates

Concerning the fourfold-coincidence-count rates in our experiment: the two entangled pairs were generated about 24 times per 10 min., while the two separable states were generated about 92 times per 10 min. We note that these numbers are the generation rates. Because of random bunching on the beam splitter, the coincidence-count rates out of the dip were half smaller. Also when local projections were applied, the rates were adequately decreased. As a result, we have obtained only about three coincidences outside the dip for the two entangled pairs per 10 min, i.e., 24/2, because of the use of the beam splitter, and a fourth of this value, because of the local polarization projections.

Experimentally measured matrices

The experimentally obtained matrices $\mathcal{R}^{(\mathrm{exp})} \equiv R^{(\mathrm{exp})} \pm \delta R^{(\mathrm{exp})}$ for the assorted states read as

$$\mathcal{R}^{(\mathrm{exp})}_{\mathrm{sep}} = \begin{bmatrix} \overline{.099} \pm .108 & \overline{.088} \pm .109 & \overline{.124} \pm .109 \\ \cdots & \overline{.034} \pm .108 & \overline{.113} \pm .108 \\ \cdots & \cdots & .980 \pm .147 \end{bmatrix}, \quad (2)$$

$$\mathcal{R}^{(\mathrm{exp})}_{\mathrm{mix}} = \begin{bmatrix} .017 \pm .031 & .006 \pm .031 & \overline{.007} \pm .031 \\ \cdots & .013 \pm .033 & .016 \pm .033 \\ \cdots & \cdots & .006 \pm .029 \end{bmatrix}, \quad (3)$$

$$\mathcal{R}^{(\mathrm{exp})}_{\mathrm{ent}} = \begin{bmatrix} .990 \pm .115 & .077 \pm .087 & .008 \pm .087 \\ \cdots & .985 \pm .110 & \overline{.013} \pm .110 \\ \cdots & \cdots & .959 \pm .079 \end{bmatrix}, \quad (4)$$

where $\overline{x} = -x$ and $\delta R^{(\mathrm{exp})}_{i,j}$ are their experimental errors.

Maximum likelihood method

To ensure the positivity of the reconstructed matrices, we use the maximum likelihood method developed for quantum state tomography (see, e.g., Ref. [1]). We find the physical matrix $R = [R_{i,j}]$, which is the closest to the experimental but unphysical matrix $R^{\mathrm{exp}} = [R^{(\mathrm{exp})}_{i,j}]$, by maximizing the logarithmic likelihood function

$$\mathcal{L} = -\sum_{1\le i\le j}^{3} \left(\frac{R^{(\mathrm{exp})}_{i,j} - R_{i,j}}{\delta R^{(\mathrm{exp})}_{i,j}}\right)^2 \quad (5)$$

subject to $0 \le r_j \le 1$ for $j = 1, 2, 3$ and $[r_1, r_2, r_3] = \mathrm{eig}(R)$. This condition is equivalent to requiring the probabilities of coincidence detections to be defined properly in any basis. Our maximum-likelihood estimates

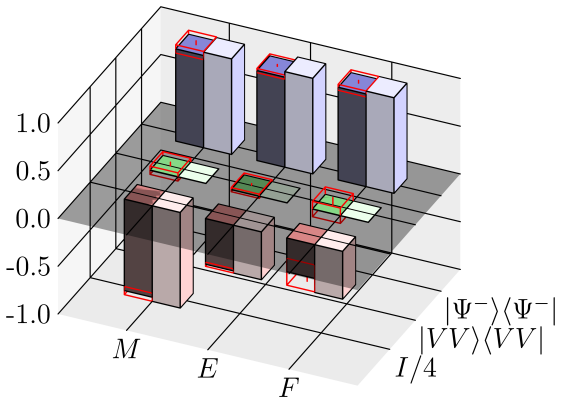

FIG. S1. Experimentally and theoretically obtained values of the Bell nonlocality measure M, entropic witness E, and fully-entangled fraction F. The bright (dark) bars correspond to theoretical (experimental) values. The associated uncertainties are marked by red frames.

read as

$$R_{\rm sep} \approx \begin{bmatrix} .008 & .008 & \overline{.086} \\ \cdots & .008 & \overline{.091} \\ \cdots & \cdots & .982 \end{bmatrix}, \quad (6)$$

$$R_{\rm mix} \approx \begin{bmatrix} .018 & .004 & \overline{.004} \\ \cdots & .015 & .011 \\ \cdots & \cdots & .010 \end{bmatrix}, \quad (7)$$

$$R_{\rm ent} \approx \begin{bmatrix} .963 & .038 & .010 \\ \cdots & .961 & \overline{.012} \\ \cdots & \cdots & .959 \end{bmatrix}. \quad (8)$$

The corresponding spectra calculated for the exact maximum likelihood estimates are $\mathrm{eig}(R_{\rm mix}) = [0.019, 0.000, 0.024]$, $\mathrm{eig}(R_{\rm ent}) = [0.919, 1.000, 0.965]$ and $R_{\rm sep} = [0.000, 0.998, 0.000]$.

The matrices R are shifted on average by a fraction of 0.19, 0.02, 0.07 of $\delta R^{(\rm exp)}$ from $R^{(\rm exp)}$ for the pure separable, maximally mixed, and singlet states, respectively. Thus, we can assume that $R^{(\rm exp)} \approx R$. The largest errors occur for the pure states. This is because the state is aligned with only one of the eigenstates for the measurement apparatus. In this case, we observe relatively low coincidence rates for the other eigenstates of the apparatus. Each matrix element $R_{i,j}$ depends on four projections onto eigenstates of $\sigma_i \otimes \sigma_j$ performed simultaneously by Bob.

Measured entanglement witnesses

Our maximum likelihood estimates were used to calculate the values of the entanglement witnesses as summarized in Fig. S1 and the Table I in the main article. The errors introduced by the setup were estimated by comparing the results of the measured etalon states ($|VV\rangle$

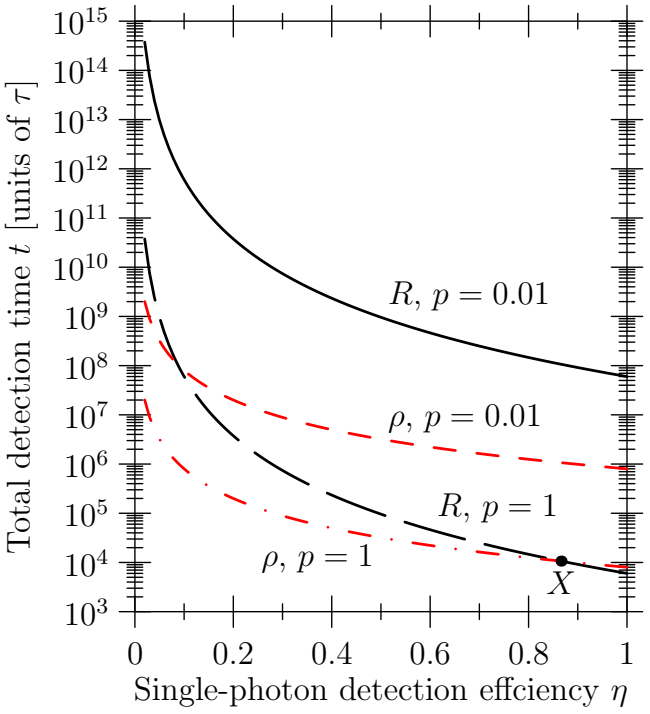

FIG. S2. Time t (in units of τ) between generating two two-photon states versus the effective single-photon detection efficiency η. This time t is required for performing 10^3 successful measurements for each element of the R matrix (in our method) and the density matrix ρ (in quantum tomography) with two photon pairs. The success rate of generating two pairs of photons from a single pump pulse is assumed to be $p^2 = 0.0001, 1$ (i.e., $p = 0.01, 1$ for a single pair generated in either forward or backward direction). The solid and long-dashed curves correspond to measuring R matrix for $p = 0.1$ and $p = 1$, respectively. The short-dashed (dashed-dotted) curves correspond to quantum tomography for $p = 0.1$ ($p = 1$). In our experiment, the repetition rate of the pump is set to $1/\tau = 80\,\mathrm{MHz}$ ($\tau = 12.5\,\mathrm{ns}$). This rate is limited by the dead time of the detectors (typically about 50 ns). However, in our experiment the possibility of a photon pair reaching a detector during its dead time can be neglected due to losses (filtering) in the setup. Measuring the R matrix, with 10^3 iterations per matrix element in a period of time of order of 1 s, would be possible in our detection setup with $\eta > 0.1$ and $p \approx 1$. In the case of a highly-efficient or deterministic two-photon source ($p = 1$), the R-matrix method can be faster than quantum tomography if $\eta > \sqrt{3}/2$. For $p = 1$ both methods are equally fast at point $X = (0.8660, 10667\tau)$, where the whole measurement of R could take less than 1 ms. However, in our proof-of-principle experiment, this time is much longer due to technological losses introduced by the setup and filtering the signal to ensure indistinguishability of the measured photons. This situation corresponds to $p\eta^2 \approx 6.4 \times 10^{-6}$ (see solid curve at $\eta = 0.0254$).

and $I/4$) with the theoretical predictions. A comparison of the total detection times versus efficiencies for our method and quantum state tomography is presented in Fig. S2.

The Werner states

The spectrum of $R_{\mathcal{W}}$ matrix of the Werner states can be expressed as $\mathrm{eig}(R_{\mathcal{W}}) \approx p^2\mathrm{eig}(R_{\mathrm{ent}}) + (1-p)^2\mathrm{eig}(R_{\mathrm{mix}})$. This is approximation is valid if $\mathrm{eig}(R_{\mathrm{ent}}) \gg \mathrm{eig}(R_{\mathrm{mix}}) \approx 0$ and the resulting $\mathrm{Tr}\sqrt{R_{\mathcal{W}}}$ is linearly dependent on the mixing parameter p [for the ideal Werner states $F = (3p-1)/2$].

* bark@amu.edu.pl
† k.lemr@upol.cz
‡ acernoch@fzu.cz
§ miran@amu.edu.pl

[1] D. F. V. James, P. G. Kwiat, W. J. Munro, and A. G. White, "Measurement of qubits," Phys. Rev. A **64**, 052312 (2001).
[2] K. Życzkowski, P. Horodecki, A. Sanpera, and M. Lewenstein, "Volume of the set of separable states," Phys. Rev. A **58**, 883–892 (1998).
[3] G. Vidal and R. F. Werner, "Computable measure of entanglement," Phys. Rev. A **65**, 032314 (2002).
[4] R. Horodecki, P. Horodecki, M. Horodecki, and K. Horodecki, "Quantum entanglement," Rev. Mod. Phys. **81**, 865–942 (2009).